PERGAMON

Pattern Recognition 35 (2002) 1559–1570

PATTERN RECOGNITION
THE JOURNAL OF THE PATTERN RECOGNITION SOCIETY

www.elsevier.com/locate/patcog

A new approach to edge detection

Z.J. Hou, G.W. Wei*

Department of Computational Science, Faculty of Science, National University of Singapore, Singapore 117543, Singapore

Received 23 March 2000; received in revised form 2 November 2000; accepted 22 June 2001

Abstract

This paper introduces the discrete singular convolution (DSC) algorithm for edge detection. Two classes of new edge detectors, DSC edge detector (DSCED) and DSC anti-noise edge detector (DSCANED), are proposed for the detection of multiscale edges. The DSCED is capable of extracting the fine details of images, whereas DSCANED is robust against noise. The combination of two classes of DSC edge detectors provides an efficient and reliable approach to multiscale edge detection. Computer experiments are carried out for extracting edge information from real images, with and without the contamination of Gaussian white noise. Sharp image edges are obtained from a variety of sample images, including those that are degraded to a peak-signal–noise-ratio (PSNR) of 16 dB. Some of the best results are attained from a number of standard test problems. The performance of the proposed algorithm is compared with many other existing methods, such as the Sobel, Prewitt and Canny detectors.

Keywords: Edge detection; Image processing; Discrete singular convolution; Multiscale

1. Introduction

The edges in an image usually refer to rapid changes in some physical properties, such as geometry, illumination, and reflectivity. Mathematically, a discontinuity may be involved in the function representing such physical properties. In practice, human perception effects play an important role in determining whether an edge exists or not. Edge detection is a key issue in image processing, computer vision, and pattern recognition. In the context of digital image processing, the concept of discontinuity does not apply and an edge may refer to systematic, rapid variation of gray-level values over number of scales. A variety of algorithms have been proposed for analyzing image intensity variation, including statistical methods [1–5], difference methods [6–8] and curve fitting methods [9–13].

Edge detection in noisy environment can be treated as an optimal linear filter design problem [14–18]. Canny [15] formulated edge detection as an optimization problem and defined an optimal filter, which can be efficiently approximated by the first derivative of Gaussian function in the one-dimensional case. Canny's filter was further extended to recursive filters [19], which provide a more efficient way for image noise filtering and edge detection.

Other edge detection methods include differentiation-based edge detection using logarithmic image processing (LIP) models [20], contrast-based methods [21], relaxation labeling techniques [22] and anisotropic diffusion [23,24]. In fact, these methods can be combined to achieve better performance. For instance, the second directional derivative edge detector proposed by Haralick [9] can be regarded as a hybrid of the differentiation method and the statistical hypothesis testing method, which leads to better performance in a noisy environment.

In the last decade, there has been renewed interest in wavelet theory, with applications in filtering,

* Corresponding author. Tel.: +65-874-6589; fax: +65-774-6756.

E-mail address: cscweigw@nus.edu.sg (G.W. Wei).

0031-3203/02/$22.00
PII: S0031-3203(01)00147-9

classification, and compression [25]. Wavelet and its associated multiresolution analysis have also been applied for the characterization of image intensity variations. Mallat et al. [26] have shown that many images can be adequately approximated by wavelet bases. Discrete wavelet transform (DWT) decomposes an image into a set of successively smaller images with different scales of resolutions. The magnitude of coefficients in different scales of the wavelet transform domain can be modified prior to carrying out the inverse wavelet transform. This procedure can selectively accentuate interesting components at the expense of undesirable ones. Equipped with wavelet analysis, one can collect quadratic filter responses at selected scales [27], so that an image edge is more reasonably identified with appropriate filter responses at a number of desired scales.

More recently, a discrete singular convolution (DSC) algorithm was proposed as a potential approach for computer realization of singular integrations [28,29]. The mathematical foundation of the algorithm is the theory of distributions [30] and wavelet analysis. Sequences of approximations to the singular kernels of Hilbert type, Abel type and delta type were constructed. In solving differential equations, the DSC approach exhibits the accuracy of a global method for integration and the flexibility of a local method for handling complex geometry and boundary conditions. In the context of image processing, DSC kernels were used to facilitate a new anisotropic diffusion operator for image restoration from noise [31]. Most recently, DSC kernels were used to generate a new class of wavelets, which include the Mexican hat wavelet as a special case [32].

The purpose of this study is to propose a new approach based on the DSC algorithm for edge detection. We illustrate this approach by using a special class of DSC kernels, the DSC kernels of delta type. In particular, DSC kernels constructed from functions of the Schwartz class are easy to use. Comparison is made between the proposed DSC detectors and the Canny detectors. Experiments indicate that the new approach is effective for image edge detection under severe Gaussian white noise.

The rest of the paper is organized as the following. In Section 2, we describe the theory and algorithm for edge detections. The theory of discrete singular distribution (DSC) is briefly reviewed. Two new classes of edge detectors are proposed for multiscale feature extraction in both normal and noisy environment. DSC edge detectors (DSCED) are constructed as fine-scale edge detectors. Moreover, DSC anti-noise edge detectors (DSCANED) are designed as coarse-scale edge detectors. The application of the present algorithm is given in Section 3. The utility is illustrated by a number of real images. Both noise free images and noisy images are treated. The performance of the proposed approach is tested by using an objective measure. The conclusion is given in Section 4.

2. Theory and algorithm

2.1. The discrete singular convolution

It is most convenient to discuss singular convolution in the context of the theory of distributions. Let T be a distribution and $\eta(x)$ be an element of the space of test functions. A singular convolution is defined as

$$F(t) = (T * \eta)(t) = \int_{-\infty}^{\infty} T(t-x)\eta(x)\,\mathrm{d}x. \tag{1}$$

Here $T(t-x)$ is a *singular kernel*. The singular convolution is the central issue for a wide range of science and engineering problems. Of particular relevance to the present study is the singular kernels of the *delta* type

$$T(x) = \delta^{(n)}(x), \quad n = 0, 1, 2, \ldots, \tag{2}$$

where δ is the delta distribution. Here the superscript denotes the nth order derivative. Although the delta distribution is called Dirac delta function, it is not a function per se. It does not even have a value anywhere. The kernel $T(x) = \delta^{(0)}(x)$ is important for interpolation and $T(x) = \delta^{(n)}(x)$ $(n = 1, 2, \ldots)$ are essential for differentiations. However, these kernels cannot directly be applied in numerical computations because of their singular nature. One method to overcome this difficulty is to construct an approximation $\{T_\alpha\}$ that converges to the singular kernel $\lim_{\alpha\to\alpha_0} T_\alpha \to T(x)$, where α_0 is a generalized limit. In the case of $T(x) = \delta(x)$, the kernel $T_\alpha(x)$ is a delta sequence kernel. With a sufficiently smooth approximation, it is useful to consider a discrete singular convolution (DSC)

$$F_\alpha(t) = \sum_k T_\alpha(t - x_k) f(x_k), \tag{3}$$

where $F_\alpha(t)$ is an approximation to $F(t)$ and x_k is an appropriate set of discrete points on which the DSC is well defined. Here, in general, $f(x)$ is not required to be a test function.

An important example of the DSC kernels is Shannon's delta kernel

$$\delta_\alpha(x) = \frac{\sin(\alpha x)}{\pi x}. \tag{4}$$

Numerically, Shannon's delta kernel is a reproducing kernel

$$f(x) = \int_{-\infty}^{\infty} f(y)\frac{\sin\pi(x-y)}{\pi(x-y)}\,\mathrm{d}y \quad \forall f \in B_\pi^2, \tag{5}$$

where $\forall f \in B_\pi^2$ indicates that, in its Fourier representation, the L^2 function f vanishes outside the

interval $[-\pi,\pi]$. Here B_π^2 is the Paley–Wiener reproducing kernel Hilbert space which is a subspace of the Hilbert space $L^2(R)$. The Paley–Wiener reproducing kernel Hilbert space has a very useful *sampling basis* $[S_k(x)=\sin\pi(x-k)/\pi(x-k),\ (k\in Z)]$, which provides a *discrete representation* of every (continuous) function in B_π^2

$$f(x)=\sum_{k\in Z} f(y_k)S_k(x) \quad \forall f\in B_\pi^2, \tag{6}$$

where symbol Z denotes the set of all integers. Eq. (6) is recognized as Shannon's sampling theorem.

2.2. DSC filters

From the point of view of signal processing, Shannon's delta kernel $\delta_\alpha(x)$ corresponds to a family of *ideal low pass filters*, each with a different bandwidth. Their corresponding wavelet expressions

$$\psi_\alpha(x)=\frac{\sin 2\alpha x-\sin\alpha x}{\pi x}, \tag{7}$$

are band pass filters. Both $\delta_\alpha(x)$ and its associated wavelet play a crucial role in information theory and theory of signal processing. However, their usefulness is limited by the fact that $\delta_\alpha(x)$ and $\psi_\alpha(x)$ are infinite impulse response (IIR) filters and their Fourier transforms $\hat{\delta}(\omega)$ and $\hat{\psi}(\omega)$ are not differentiable. Computationally, $\phi(x)$ and $\psi(x)$ do not have finite moments in the coordinate space; in other words, they are de-localized. This non-local feature in coordinate is related to the bandlimited character in the Fourier representation according to the Heisenberg uncertainty principle. To improve the asymptotic behavior of Shannon's delta kernel in the coordinate representation, a regularization procedure can be used and the resulting DSC kernel in its discretized form can be expressed as

$$\delta_{\sigma,\alpha}(x-x_k)=\frac{\sin(\pi/\Delta)(x-x_k)}{(\pi/\Delta)(x-x_k)}\mathrm{e}^{-(x-x_k)^2/2\sigma^2} \quad \sigma>0. \tag{8}$$

Here, it is understood that $\alpha=\pi/\Delta$ and expression (8) is used in discrete computations exclusively.

An immediate benefit of the regularized Shannon's delta kernel, Eq. (8), is that its Fourier transform is infinitely differentiable. Both Shannon's delta kernel and the regularized Shannon's delta kernel are plotted in Fig. 1. Qualitatively, all kernels oscillate in the coordinate representation. Shannon's delta kernel has a long tail which is proportional to $1/x$. Whereas, the regularized kernels decay much faster, especially when σ is very small. In the Fourier representation, Shannon's delta kernel is the ideal low pass filter, which is discontinuous at $\omega=\frac{1}{2}$. In contrast, all regularized kernels have an "optimal" shape in their frequency responses. Of course, they all reduce

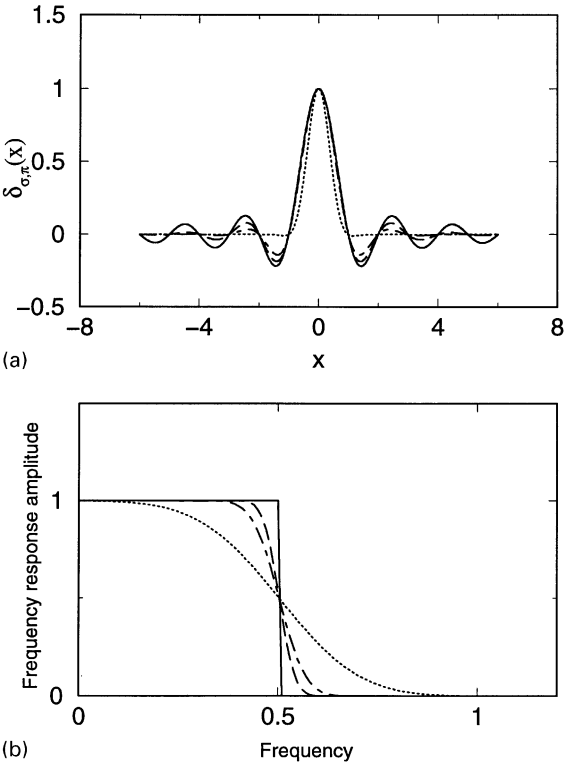

Fig. 1. Graphs of $\delta_{\sigma,\pi}(x)$ and its frequency response. The dotted line: $\sigma=1$; the dot dashed line: $\sigma=3$; the dashed line: $\sigma=5$; the solid line: $\sigma=\infty$.

to Shannon's delta filter at the limit

$$\lim_{\sigma\to\infty}\delta_{\sigma,\pi}(x)=\lim_{\sigma\to\infty}\frac{\sin\pi x}{\pi x}\mathrm{e}^{-x^2/2\sigma^2}=\frac{\sin\pi x}{\pi x}. \tag{9}$$

2.3. DSC edge detectors

To construct edge detectors, we consider a one-dimensional, nth order DSC kernel of the delta type

$$\delta_{\sigma,\alpha}^{(n)}(x-x_k), \quad n=0,1,2,\ldots\ .$$

Here $\delta_{\sigma,\alpha}^{(0)}(x-x_k)=\delta_{\sigma,\alpha}(x-x_k)$ is a DSC filter. The expression given in Eq. (8) is an example of the DSC filters and many other examples are given in Ref. [28]. The derivatives $\delta_{\sigma,\alpha}^{(n)}(x_m-x_k)$ $(n=1,2,\ldots)$ are obtained by differentiation

$$\delta_{\sigma,\alpha}^{(n)}(x_m-x_k)=\left[\left(\frac{\mathrm{d}}{\mathrm{d}x}\right)^n\delta_{\sigma,\alpha}(x-x_k)\right]_{x=x_m}, \tag{10}$$

and can be regarded as high-pass filters. The filters for $n=1$–3 and their frequency responses are plotted in Fig. 2. It is seen that filters corresponding to the derivatives of Shannon's delta kernel decay slowly as x increases, whereas, regularized filters are functions of the Schwartz class and have controlled residue amplitude at

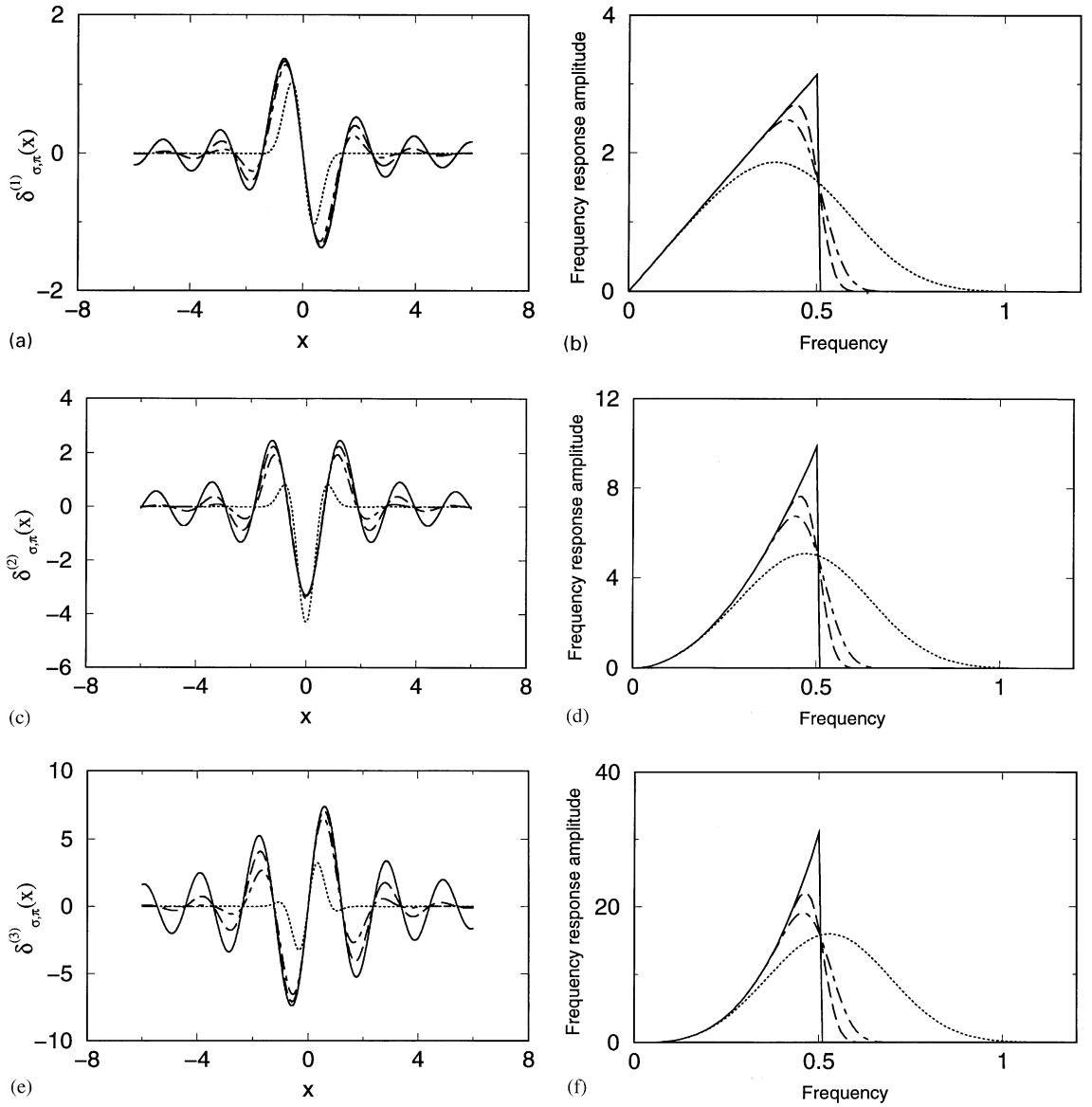

Fig. 2. High-pass filters $\delta^{(n)}_{\sigma,\pi}(x)$ and their frequency responses. The dotted line: $\sigma = 1$; the dot dashed line: $\sigma = 3$; the dashed line: $\sigma = 5$; the solid line: $\sigma = \infty$. (a) and (b): $n = 1$; (c) and (d): $n = 2$; (e) and (f): $n = 3$.

large x values. In the Fourier representation, the derivatives of Shannon's delta kernel are discontinuous at certain points. In contrast, the derivatives of regularized kernels are all continuous and can be made as close to those of Shannon's as one wishes.

Fig. 2 also illustrates the impact of parameter σ on the filters in the time–frequency domain. For fixed α, the larger the σ value is, the slower the filters will decay in the time domain. As a result, the truncation error increases for numerical computations. In the frequency domain, however, these filters become more localized with the increase of σ. But difference in σ values has little impact on the low frequency responses of various filters. To balance the localization of a filter in both the time and frequency domains, an optimal σ is required and can be attained for a given practical problem.

Fig. 3 shows the influence of parameter α on the frequency response of $\delta^{(1)}_{\sigma,\alpha}$ for a given σ. It is seen that the frequency response is very sensitive to the change of α value. With the decrease of α, the peak of frequency response moves from the high frequency region to the low frequency one. At the limit of $\alpha \to 0$, the frequency

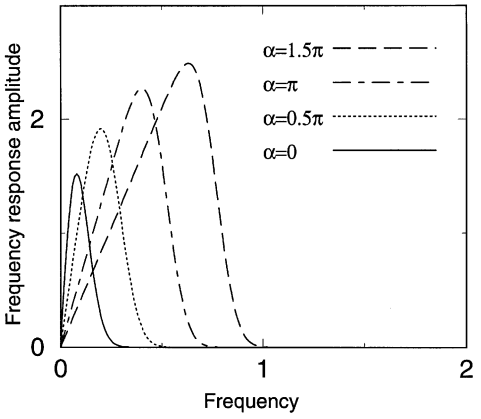

Fig. 3. Frequency response of DSCED[1] with different α values ($\sigma = 2$).

response localizes at a very low frequency region. Obviously, the DSC parameter α can be utilized to achieve an optimal frequency selection in a practical application. For example, in many problems, the object to be processed may be corrupted by noise whose frequency distribution mainly concentrates in the high frequency region. Therefore, a small α value can be used to avoid the noise corruption.

For noise free images, the nth order fine-scale DSC edge detector (DSCED^n) is given by

$$\begin{aligned}&\mathrm{DSCED}^n(x_i, y_j)\\ &= \left| \sum_{k=-W_n}^{W_n} \delta^{(n)}_{\sigma_n,\alpha_n}(x_i - x_k) I(x_k, y_j) \right|\\ &\quad + \left| \sum_{l=-W_n}^{W_n} \delta^{(n)}_{\sigma_n,\alpha_n}(y_j - y_l) I(x_i, y_l) \right|, \quad n = 1, 2, \ldots,\end{aligned} \tag{11}$$

where I is a digital image. In principle, all derivatives ($n = 1, 2, \ldots$) can be employed for edge detection and in general, an appropriate linear combination of them may be required because image edges can exhibit various shapes. Nevertheless, in most situations, DSCED[1] is quite sufficient and very easy to implement. These edge detectors are capable of extracting fine details. However, they perform less well for images that are corrupted with much noise.

Due to the possible presence of noise, the definition of image edge is not unique and finding edge by differentiation is an ill-posed problem in a digital image. Essentially, the differential operator is defined based on continuous and differentiable functions. Its discrete version, the difference operation (or difference operator as referred in the literature), is strictly applicable only to those sets of discrete values that are attained by the appropriate discretization of the original continuous and differentiable functions. Therefore, we define edges at different levels of scales and we call them multiscale edges. The concept of multiscale edges has an advantage that one can locate an edge at selected scale which is comparable to the physical extension of the feature. A fine-scale edge detector, as given in Eq. (11), is capable of extracting features at all scales, though it is sensitive to noise. However, a coarse-scale edge detector is not too sensitive to fine details and is capable of performing well under noisy conditions. One way to extract the present multiscale edges is to use the wavelet multiresolution analysis. Another practical way for detecting multiscale edges is to construct edge detectors by a combination of filtering and edge detection. In the present work, the nth order DSC anti-noise edge detector (DSCANED^n), or the nth order coarse-scale DSC edge detector, is proposed as

$$\begin{aligned}&\mathrm{DSCANED}^n(x_i, y_j)\\ &= \left| \sum_{k=-W_n}^{W_n} \sum_{l=-W_0}^{W_0} \delta^{(n)}_{\sigma_n,\alpha_n}(x_i - x_k)\, \delta^{(0)}_{\sigma_0,\alpha_0}(y_j - y_l) I(x_k, y_l) \right|\\ &\quad + \left| \sum_{k=-W_0}^{W_0} \sum_{l=-W_n}^{W_n} \delta^{(0)}_{\sigma_0,\alpha_0}(x_i - x_k)\, \delta^{(n)}_{\sigma_n,\alpha_n}(y_j - y_l) I(x_k, y_l) \right|,\\ &\qquad n = 1, 2, \ldots .\end{aligned} \tag{12}$$

Note that the differentiation matrices in Eqs. (11) and (12) are, in general, banded. This is advantageous in large-scale computations.

Although the present DSCED^n and DSCANED^n are designed as fine and coarse edge detectors, respectively, they operate on the same grid. It is possible to carry out the operations after appropriate down samplings. This multiscale procedure may be better for detecting edges under noisy conditions. For simplicity, the details of this procedure are not presented in this paper.

3. Results and discussion

To explore the utility and demonstrate the efficiency of the proposed approach, we carry out computer experiments on gray-level images. To this end, we select a few classes of standard images, which are either natural or human-made. A summary of the images used in the present study is plotted in Fig. 4. The golfcar, boat and pitcher images are non-textured human-made images and the tire is a textured human-made image. The egg and pepper images are natural and non-textured images, and the pinecone image is a natural and textured image. The cameraman, Lena and Barbara images are figure images, of which the Barbara image contains line textures. The square is a synthetic image. The settings of these images vary from in-door scenes to out-door views. The

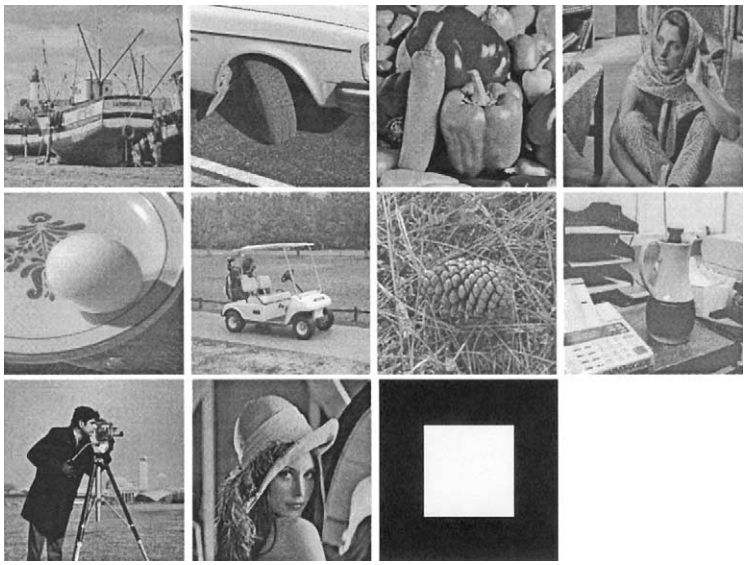

Fig. 4. A collection of sample images, where the first eight images are of the size of 512×512 and the last three are of 256×256. The first ten images are real ones and the last one is synthetic.

resolution of all images is 8-bit per pixel. The first eight images are of the size of 512×512 pixels, while the last three images are of 256×256. For definiteness and simplicity, we set the parameter $W = 2$ for all experiments in this section.

Most edge detection techniques utilize a post-processing thresholding immediately after feature extraction to thin and/or extend edge contours. There are many well-established thresholding [33,34] and edge thinning techniques. In the present work, the edge detection consists of two steps: edge magnitude calculation, and thresholding. For simplicity, a fixed threshold is used in the experiments, although there are adaptive thresholding techniques that could be implemented. In general, there is no definite "rule" to select a threshold for edge detection. A useful way is to "tune" the threshold such that the resulting edge images have the same percentage of pixels in gradient images that are classified as edge pixels. Unfortunately, there is no definite rule to determine the percentage for a real image. A common practice is to assume the percentage of edge pixels is about 5–10% [20] for a normal image. In the present study, we set the percentage to 9%. The procedure described here is also applied for the implementation of other standard edge detectors, which are used for comparison in the present study.

In the rest of this section, we conduct three groups of computer experiments to test the proposed approach. Group one is designed to investigate the performance of the present algorithm on the edge detection of clean images. Group two is to examine the ability of the present algorithm on extracting edges from noisy images. The last group is designed to objectively compare the performances of different edge detectors by using a computer generated image. They are, respectively, described in the following three subsections. A brief discussion is given in the last subsection.

3.1. Clean images

In this subsection, we examine the performance of the fine-scale edge detectors, DSCED[1]. The DSCED[1] used here is a 5×1 mask. Two conventional approaches, the Sobel detector and the Prewitt detector, are also employed for comparison. It is well-known that both the Sobel and Prewitt detectors are constructed by using the finite difference in one direction in association with a low-pass filter in the normal direction for denoising.

Fig. 5 presents a comparison of the performance of five edge detectors on the sample images. Here, the first three columns are, respectively, obtained by using the DSCED[1] method with different parameters (Column 1: $\sigma_1 = 3,\ \alpha_1 = 1.5$; Column 2: $\sigma_1 = 1,\ \alpha_1 = 1.5$; Column 3: $\sigma_1 = 1,\ \alpha_1 = 0.4$). The performance of the Sobel and Prewitt detectors are given in the fourth and fifth columns, respectively. From Fig. 5, we can see the impact of the parameters on the performance of DSCED[1]. The edge map of Column 1 is much sharper than that of Column 2. This is due to the fact that a smaller σ_1 value leads to larger frequency response at the high frequency region, as shown in Fig. 2b. As a result, unwanted noise-like fine structures are produced in Column 2.

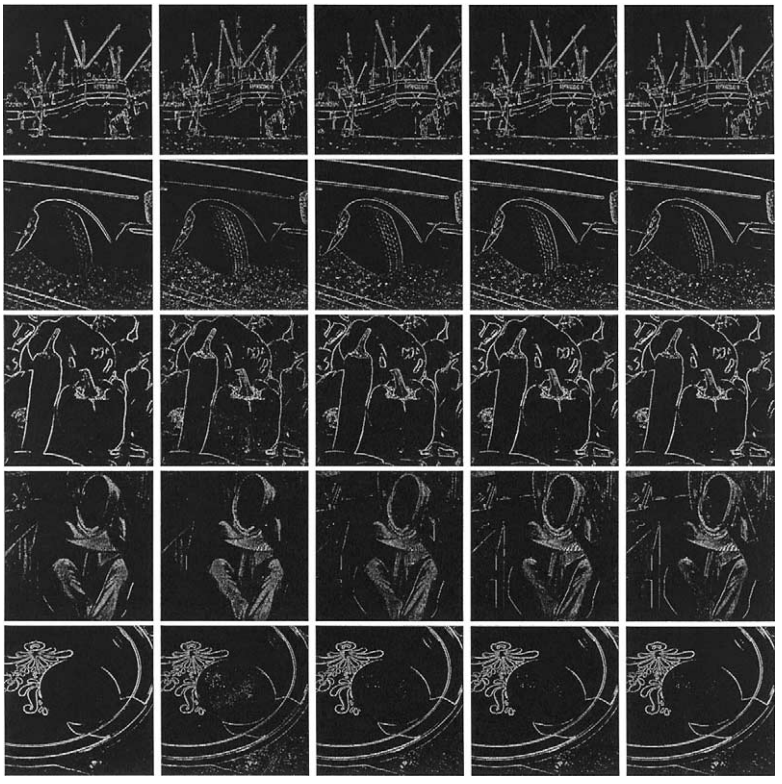

Fig. 5. Edge images obtained by using different detectors. Columns 1–3 are obtained by using the DSCED[1] with different parameters (column 1: $\sigma_1 = 3,\ \alpha_1 = 1.5$, column 2: $\sigma_1 = 1,\ \alpha_1 = 1.5$, column 3: $\sigma_1 = 1,\ \alpha_1 = 0.4$). Column 4 is obtained by using the Sobel detector and column 5 by the Prewitt detector.

As seen from Fig. 3, a smaller α_1 value leads to a narrow band frequency response. Thus, tuning α_1 is an alternative way to improve the performance of DSCED[1]. The effect of α_1 can be observed by a comparison between Columns 2 and 3. Indeed, the performance of DSCED[1] is improved generally in Column 3 by using a smaller α_1 value. The performance of DSCED[1] is further compared with that of standard methods, presented in the last two columns. The Sobel detector (Columns 4) and Prewitt detector (Column 5) provide similar results. The visual differences between these results and those of DSCED[1] in Columns 1 and 3 are marginal. Both the Sobel and Prewitt detectors are two-dimensional (3×3), whereas the DSC detectors are one-dimensional (5×1). Therefore, the DSC detectors are slightly more efficient for edge detection of these images.

It is noted that none of the above-mentioned five edge detectors resolves the facial feature of the Barbara image, which is a well-known difficult case. To illustrate the potential of the DSC detectors, we also conduct two tests by using DSCANED[1] which couples a high-pass filter with a low-pass one. The DSCANED[1] parameters are chosen as $\sigma_1 = 2,\ \alpha_1 = 0.2,\ \sigma_0 = 3,\ \alpha_0 = 0,\ W_n = 2,\ n = 0, 1$. These results are depicted in Fig. 6, along with those obtained by using the Sobel and Prewitt detectors. Clearly, the DSC detector gives rise to excellent facial features for the Barbara image.

3.2. Noisy images

To investigate the performance of the DSC algorithm under noisy environment, we consider a number of low grade images. Fig. 7 presents a summary of the noisy images, which are generated by adding independently, identically distributed (i.i.d.) Gaussian noise, and the peak-signal–noise-ratio (PSNR) for each image is 16 dB. Fig. 8 illustrates the resulting edge images detected from noisy environment, obtained by DSCANED[1] (Column 1), the Sobel detector (Column 2) and the Prewitt detector (Column 3). The effect of noise is significant and the "edges" reflecting small illumination changes are invisible. For definiteness and simplicity, DSCANED[1] parameters remain the same as those specified in the last subsection. It is possible that other combinations of the parameters could deliver similar results and the DSCANED[1] parameters could be further optimized to obtain a global optimal. A discussion of such a global optimization procedure is beyond the scope of the

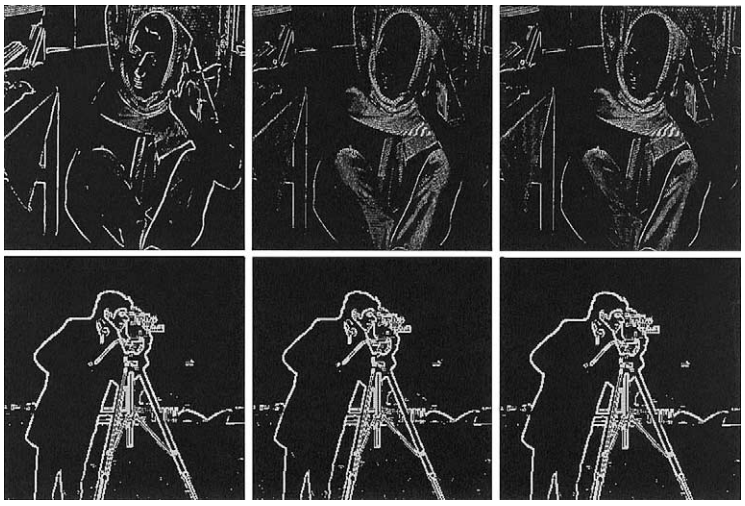

Fig. 6. A comparison of edge images obtained by using different detectors. Column 1: the DSCANED[1]; column 2: the Sobel detector; column 3: the Prewitt detector.

Fig. 7. A collections of noisy sample images (PSNR = 16 dB).

present work, and the interested readers are referred to Ref. [15].

In general, the detected edges are blurred due to the presence of noise. The two conventional detectors, the Sobel and Prewitt, detect not only spatially extended edges, but also many spurious features due to noise. As a result, the contrast of their edge images is poor. In contrast, much sharper edge images are successfully attained by the DSC detector, as shown in Column 1 of Fig. 8. The difference in contrast stems from the fact that the DSCANED[1] detects edges at a coarse scale, in which the high frequency noise has been remarkably smoothed out.

As mentioned in the introduction, the Canny detector [15] was formulated as an optimization problem for being used under noise environment. It was pointed out by Srinivasan et al. [35] that the Canny detector can be efficiently approximated by the following two filters [35]:

$$C_1 = -\frac{x}{\sigma^2} e^{-(x^2+y^2)/2\sigma^2}, \tag{13}$$

$$C_2 = -\frac{y}{\sigma^2} e^{-(x^2+y^2)/2\sigma^2}, \tag{14}$$

which represent, respectively, the edge detectors along the horizontal and vertical directions. The parameter is taken as $\sigma = 1.5$, which, as suggested by other researchers [35,36], is nearly optimal in association with a 5×5 mask. The resulting edge images are included in Column 4 of Fig. 8 for a comparison. Obviously, there is no visual difference between those obtained by using the DSC detector and the Canny detector. These experiments indicate the performance of the DSC based edge detector is as good as that of the Canny detector.

3.3. An objective comparison

To validate the DSC detector further, we present an alternative evaluation in this subsection. Edge detection systems could be compared in many ways. For example, the image gradients may be compared visually [36],

Fig. 8. Edge images of the noisy sample images, column 1–4 are obtained by using, respectively, the DSCANED[1], the Sobel detector, the Prewitt detector and the Canny detector.

where an edge image is evaluated by a group of people and the average score could be an index of quality. For synthetic images, where the exact location of edges is known, Abdou and Pratt [37] proposed a figure of merit to objectively evaluate the performance of edge detectors. Their figure of merit is defined as

$$F = \frac{1}{\max(N_I, N_D)} \sum_{i=1}^{N_D} \frac{1}{1 + \xi d_i^2}, \tag{15}$$

where d_i is the distance between a pixel declared as edge point and the nearest ideal edge pixel, ξ is a penalty constant, N_I and N_D are the numbers of ideal and detected edge pixels respectively. It is a common practice to evaluate the performance of an edge detector for synthetic images by introducing random noise in the images. A plot of F against the peak-signal–noise-ratio gives the degradation in the performance of the detector. The value of F is less than or equal to 1. The larger the value, the better the performance.

Performance comparison is based on a synthetic square image, as shown in Fig. 6. The figure of merit F for each of the methods studied is calculated with respect to different PSNR, and the results are plotted in Fig. 9. When the noise level is low, the F values are very close to 1 and the performances of all the four detectors are

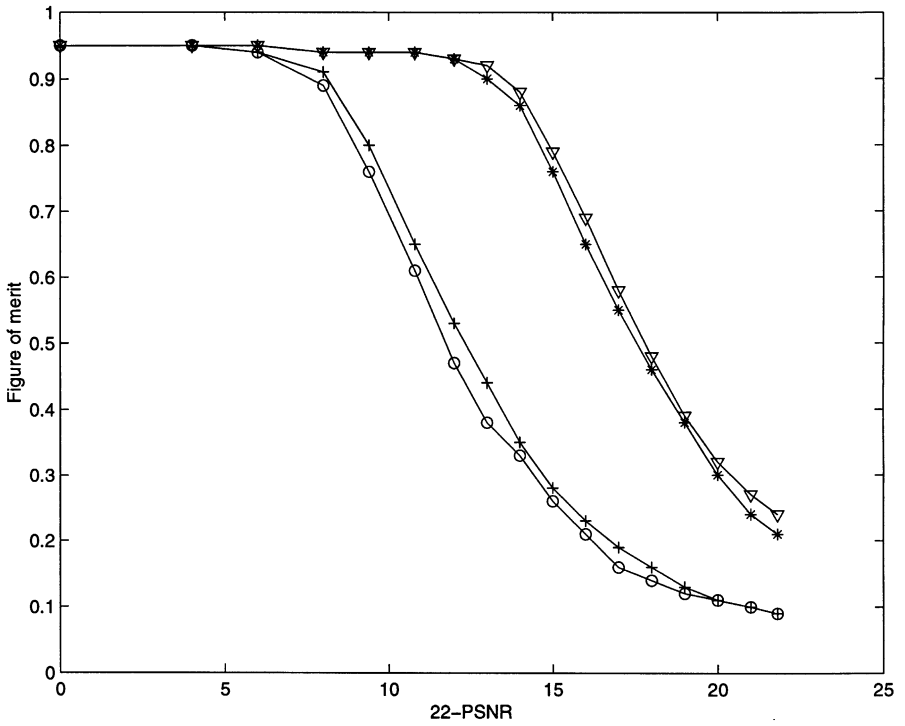

Fig. 9. The figure of merit for the synthetic square image. Triangle: the DSCANED[1]; star: the Canny detector; plus: the Prewitt detector; circle: the Sobel detector.

very satisfactory. With the increase of the noise level, the F values of two difference detectors decrease, and are less than 0.5 when PSNR is about 10 dB. In contrast, the Canny detector and the DSC detector achieve large F values over the domain of interest, suggesting their superiority to other two detectors. It is noted that the performance of ANDSCED[1] is better than that of the Canny detector for small PSNR values.

3.4. Discussion

In the presence of noise, the direct application of the differentiation operation in edge detection will encounter difficulty, as illustrated by the preceding experiments. The differentiation operation is sensitive to noise and the problem is mathematically ill-posed. To offset the effect of noise, a direct approach is to remove noise before the differentiation, usually by convolving the raw input image with a Gaussian function, which leads to the well-known Marr's detector [27]. This problem can also be solved by using regularization techniques developed for dealing with mathematically ill-posed problems [14]. Poggio et al. [38] proved that the variational formulation of Tikhonov regularization leads to a Gaussian-like convolution filter. In the present method, the idea to deal with noise basically falls into this framework, i.e. taking differentiation after a low-pass filter convolution.

It is well-known that the performance of the Canny detector depends on the computational bandwidth W and standard deviation σ. These parameters can be utilized to obtain edges which is optimized with respect to the space of parameters ($\sigma \in R^+, W \in Z^+$) for each given image. In particular, the parameter σ gives rise to excellent time–frequency localization. However, the Canny filter does not provide much freedom for frequency selection. In contrast to the Canny detector, the DSC detector has one more parameter, α, which is very efficient for frequency selection as shown in Fig. 3. Thus, DSC detector should perform at least as well as the Canny detector.

Both the Canny and DSC detectors have a parameter σ_n which affects significantly the time–frequency localization of the filter, as can be seen from Fig. 2. The Gaussian factor determines the regularity and smoothness of the DSC kernel and can be used to suppress spurious oscillations, i.e., the Gibbs phenomenon, which is unwanted in many applications, such as image processing, audio filtering and numerical computation. Appropriate choice of σ_n can judiciously balance between the degree

of noise removal and fine feature detection, and improve the overall performance.

The DSC detector has an extra parameter, α_n, which controls DSC filter frequency selection as shown in Fig. 3. Experiments in Section 3.1 indicated that, when α_n decreases, fine details are smoothed out and main edge structures appear significant. This property can be utilized to deal with images corrupted with color noise, for which the Canny detector is not the best choice. The ability of frequency selection is important to many practical applications. Since it has one more parameter to be optimized, the DSC algorithm is a potential method for more complicated tasks. Optimization of DSC parameters in more general conditions will be conducted in our future study.

4. Conclusion

This paper introduces the discrete singular convolution (DSC) algorithm [28] for edge detection. A number of DSC (low-pass) filters are proposed in the context of distribution theory. A family of regularized DSC kernels are constructed for denoising and data interpolation. Edge detection is analyzed as a multiscale process, in which the compatibility between physical extension and the scale of a detector is emphasized. Two classes of DSC edge detectors are constructed in the present work. One class is for clean images, the fine-scale DSC edge detector (DSCED^n), and the other for noisy images, the coarse-scale DSC anti-noise edge detector (DSCANED^n). The combined use of the two DSC edge detectors make the present algorithm efficient for edge detection in a variety of practical situations. The performance of the proposed algorithm is compared with many other existing methods, such as the Sobel, Prewitt and Canny detectors. The Canny detector can be optimized with respect to the filter length and time–frequency localization, whereas, the DSC detector can be optimized with respect to one more parameter, α, which plays the role of frequency selection. Experiments on a variety of images have been carried out with some selected DSC parameters, and the performance of DSC detectors is at least as good as that of the Canny detector.

Acknowledgements

This work was supported in part by the National University of Singapore. The authors are grateful to the referee for valuable comments and suggestions.

References

[1] D. Stern, L. Kurz, Edge detection in correlated noise using Latin squares models, Pattern Recognition 21 (1988) 119–129.

[2] J. Haberstroh, L. Kurz, Line detection in noisy and structured background using Graco-Latin squares, CVGIP: Graphical Models Image Process. 55 (1993) 161–179.

[3] N.E. Nahi, T. Assefi, Bayesian recursive image estimation, IEEE Trans. Comput. 7 (1972) 734–738.

[4] F.R. Hansen, H. Elliot, Image segmentation using simple Markov field models, Comput. Graphics Image Process. 20 (1982) 101–132.

[5] J.S. Huang, D.H. Tseng, Statistical theory of edge detection, Comput. Vision Graphics Image Process. 43 (1988) 337–346.

[6] J.M.S. Prewitt, Object enhancement and extraction, in: B.S. Lipkin, A. Rosenfeld (Eds.), Picture Processing and Psychopictorics, Academic Press, New York, 1970.

[7] R. Kirsh, Computer determination of the constituent structure of biological images, Comput. Biomed. Res. 4 (1971) 314–328.

[8] D. Marr, E. Hidreth, Theory of edge detection, Proc. Roy. Soc. London PAMI-6 (1984) 58.

[9] R.M. Haralick, Digital step edges from zero crossing second directional derivatives, IEEE Trans. Pattern Anal. Mach. Intell. PAMI-6 (1984) 58–68.

[10] M.H. Huechel, An operator which locates edges in digitized pictures, J. Assoc. Comput. Mach. 18 (1971) 113–125.

[11] R.M. Haralick, L. Watson, A facet model for image data, Comput. Graphics Image Process. 15 (1981) 113–129.

[12] V. Nalwa, T.O. Binford, On detecting edges, IEEE Trans. Pattern Anal. Mach. Intell. PAMI-6 (1984) 58–68.

[13] V.S. Nalwa, T.O. Binford, On detecting edges, IEEE Trans. Pattern Anal. Mach. Intell. PAMI-8 (1986) 699–714.

[14] V. Torre, T. Poggio, On edge detection, IEEE Trans. Pattern Anal. Mach. Intell. PAMI-2 (1986) 147–163.

[15] J. Canny, A computational approach to edge detection, IEEE Trans. Pattern Anal. Mach. Intell. PAMI-8 (1986) 679–698.

[16] T.D. Sanger, Optimal unsupervised learning in a single layer feedforward neural network, Neural Networks 2 (1989) 459–473.

[17] B.S. Manjunath, R. Chellappa, A unified approach to boundary perception: edges, textures and illusory contours, IEEE Trans. Neural Networks 4 (1993) 96–108.

[18] S. Sarkar, K.L. Boyer, On optimal infinite impulse response edge detection filters, IEEE Trans. Pattern Anal. Mach. Intell. PAMI-13 (1991) 1154–1171.

[19] R. Deriche, Optimal edge detection using recursive filtering, Proceedings of the First International Conference on Computer Vision, London, 1987.

[20] G. Deng, J.-C. Pinoli, Differentiation-based edge detection using the logarithmic image processing model, J. Math. Imaging vision 8 (1998) 161–180.

[21] R.P. Johnson, Contrast based edge detection, Pattern Recognition 23 (1990) 311–318.

[22] S.S. Iyengar, W. Deng, An efficient edge detection algorithm using relaxation labeling technique, Pattern Recognition 28 (1995) 519–536.

[23] P. Perona, J. Malik, Scale-space and edge detection using anisotropic diffusion, IEEE Trans. Pattern Anal. Mach. Intell. 12 (1990) 629–639.

[24] M.J. Black, G. Sapiro, D.H. Marimont, D. Heeger, Robust anisotropic diffusion, IEEE Trans. Image Process. 7 (1998) 421–432.
[25] S. Mallat, S. Zhong, Characterization of signals from multiscale edges, IEEE Trans. Pattern Anal. Mach. Intell. 14 (1992) 710–732.
[26] S. Mallat, Zero-crossings of a wavelet transform, IEEE Trans. Inform. Technol. IT-37 (1991) 1019–1033.
[27] D. Marr, E. Hildreth, Theory of edge detection, Proc. Roy. Soc. B207 (1980) 187–217.
[28] G.W. Wei, Discrete singular convolution for the solution of the Fokker–Planck equations, J. Chem. Phys. 110 (1999) 8930–8942.
[29] G.W. Wei, A unified approach for the solution of the Fokker–Planck equation, J. Phys. A: Math. Gen. 33 (2000) 4935–4953.
[30] L. Schwartz, Théore des Distributions, Hermann, Paris, 1951.
[31] G.W. Wei, Generalized Perona–Malik equation for image restoration, IEEE Signal Process. Lett. 6 (1999) 165–168.
[32] G.W. Wei, Wavelets generated by using discrete singular convolution kernels, J. Phys. A: Math. Gen. 33 (2000) 8577–8596.
[33] T. Peli, D. Malah, A study of edge detection algorithms, Comput. Graphics Image Process 20 (1982) 1–21.
[34] L. Hertz, R.W. Schafer, Multilevel thresholding using edge matching, Comput. Vision Graphics Image Process 44 (1988) 279–295.
[35] V. Srinivasan, P. Bhatia, S.H. Ong, Edge detection using neural network, Pattern Recognition 27 (1994) 1653–1662.
[36] M.D. Heath, S. Sarkar, T. Sanocki, K.W. Bowyer, A robust visual method for assessing the relative performance of edge-detection algorithms, IEEE Trans. Pattern Anal. Mach. Intell. 19 (1997) 1338–1359.
[37] I.E. Abdou, W.K. Pratt, Quantitative design and evaluation of enhancement/thresholding edge detectors, Proc. IEEE. 69 (1979) 753–763.
[38] T. Poggio, H. Voorhees, A. Yuille, A regularized solution to edge detection, J. Complexity 4 (1988) 106–123.

About the Author—ZUJUN HOU is currently a Ph.D. candidate at the Department of Computational Science, National University of Singapore. His present research interests include image and signal processing, and pattern recognition.

About the Author—GUO WEI WEI received his Ph.D. degree from the University of British Columbia, in 1996. He was a Canadian NSERC postdoctoral fellow and research assistant professor at the University of Houston before joining the Department of Computational Science, National University of Singapore, in 1998, where he is currently an associate professor.

Dr. Wei is a member of IEEE, SIAM and APS. His research interests include computational methodology and its applications, and nonlinear dynamics.